

ARTICLE

Open Access

Autism-associated miR-873 regulates *ARID1B*, *SHANK3* and *NRXN2* involved in neurodevelopment

Jing Lu¹, Yan Zhu¹, Sarah Williams², Michelle Watts³, Mary A. Tonta¹, Harold A. Coleman¹, Helena C. Parkinson¹ and Charles Claudianos^{1,4}

Abstract

Autism spectrum disorders (ASD) are highly heritable neurodevelopmental disorders with significant genetic heterogeneity. Noncoding microRNAs (miRNAs) are recognised as playing key roles in development of ASD albeit the function of these regulatory genes remains unclear. We previously conducted whole-exome sequencing of Australian families with ASD and identified four novel single nucleotide variations in mature miRNA sequences. A pull-down transcriptome analysis using transfected SH-SY5Y cells proposed a mechanistic model to examine changes in binding affinity associated with a unique mutation found in the conserved 'seed' region of miR-873-5p (rs777143952: T > A). Results suggested several ASD-risk genes were differentially targeted by wild-type and mutant miR-873 variants. In the current study, a dual-luciferase reporter assay confirmed miR-873 variants have a 20-30% inhibition/dysregulation effect on candidate autism risk genes *ARID1B*, *SHANK3* and *NRXN2* and also confirmed the affected expression with qPCR. In vitro mouse hippocampal neurons transfected with mutant miR-873 showed less morphological complexity and enhanced sodium currents and excitatory neurotransmission compared to cells transfected with wild-type miR-873. A second in vitro study showed CRISPR/Cas9 miR-873 disrupted SH-SY5Y neuroblastoma cells acquired a neuronal-like morphology and increased expression of ASD important genes *ARID1B*, *SHANK3*, *ADNP2*, *ANK2* and *CHD8*. These results represent the first functional evidence that miR-873 regulates key neural genes involved in development and cell differentiation.

Introduction

Autism spectrum disorders (ASD) are characterised by impaired social interaction, communication deficits, restricted and repetitive behaviour, and affect 1–2% of the world population. Extensive research has been conducted to identify the genetic causes of ASD with literally hundreds of genes now linked to ASD risk¹. Currently, there are 913 genes represented in the Human Gene Module from Simons Foundation Autism Research Initiative (SFARI), a comprehensive resource on ASD genetics². Although there are few common mutations of high

frequency, many rare variations occur in risk genes associated with neurodevelopment and synapse development³. Among them, *SHANK3* encodes a notable protein scaffolding molecule that has been well studied in animal models; genetic disruption of which, results in autistic-like behaviours and neuronal morphologic deficits⁴.

Although significant efforts have been made to examine the role of DNA variations found in protein coding genes, there remains a paucity of knowledge concerning the large number of variations detected in noncoding DNA including microRNAs (miRNAs) and their target sites in mRNAs⁵. MiRNAs are short (~22 nucleotides) noncoding RNAs that regulate gene expression at all known levels of cell development, including the nervous system^{6–9}, and are thought to play a vital role in autism^{10–12}. Unfortunately, there is little direct functional evidence to support this assumption. The relationship between gene expression and

Correspondence: Jing Lu (jing.lu2@monash.edu) or Charles Claudianos (Charles.Claudianos@anu.edu.au)

¹Monash Biomedicine Discovery Institute, Monash University, Melbourne, VIC 3800, Australia

²Monash Bioinformatics Platform, Monash University, Melbourne, VIC 3800, Australia

Full list of author information is available at the end of the article

© The Author(s) 2020



Open Access This article is licensed under a Creative Commons Attribution 4.0 International License, which permits use, sharing, adaptation, distribution and reproduction in any medium or format, as long as you give appropriate credit to the original author(s) and the source, provide a link to the Creative Commons license, and indicate if changes were made. The images or other third party material in this article are included in the article's Creative Commons license, unless indicated otherwise in a credit line to the material. If material is not included in the article's Creative Commons license and your intended use is not permitted by statutory regulation or exceeds the permitted use, you will need to obtain permission directly from the copyright holder. To view a copy of this license, visit <http://creativecommons.org/licenses/by/4.0/>.

large copy number variations (CNVs) containing miRNAs has also been linked with ASD. A recent study showed that miR-137 targets 3'-untranslated region (3'UTR) of the candidate autism gene *RORA*¹³, but there has yet to be a definitive association of DNA variation of any specific miRNA with ASD¹⁴.

Current evidence suggests miRNAs usually bind to the 3'UTR of the target mRNAs to regulate protein synthesis¹⁵. The first 2–8 nucleotides are generally required for miRNA binding and thus termed as a 'seed region'; however, a single nucleotide variation (SNV) in a mature miRNA sequence may also change the stability of its precursor miRNA hairpin, or alter the mature miRNA targeting specificity¹⁵. We previously conducted high-efficiency whole-exome sequencing of Australian families with ASD ($N = 128$; 48 ASD cases and 80 parents)^{5,16} and recently reported a landmark noncoding DNA sequence analysis associated with this autism cohort. Among the many sequence variations found to occur in regulatory DNA regions of the genome, we identified four rare SNVs within mature miRNA sequences. Of interest was an inherited SNV (rs777143952; T > A) of miR-873-5p (gene ID: 100126316) found in an idiopathic ASD case. This individual inherited this miR-873 mutation from an unaffected father together with a putative disruptive *NRXNI* coding mutation (chr2:50847195; G > A; NM_004801: exon8:c.C1285T;p.P429S) from a mother diagnosed with broader autism phenotype (BAP)^{5,16}. *NRXNI* is a notable autism risk gene, deletions and disruptions of which have been reported in several ASD cases^{17–19}. MiR-873 is located within an intron of the neural gene *LINGO2*, which is highly expressed in the brain²⁰, not surprisingly, miR-873 is also highly expressed in many brain regions²¹. For this miR-873 mutation, the maximum population allele frequency is 0.000007130²². MiR-873 is very conserved and it was annotated on 17 species in miRbase²³. Interestingly, miR-873 is also found to be downregulated in brains with glioblastoma tumours²⁴ and with learning difficulties linked to a chromosomal microdeletion that includes miR-873²⁵. As previously stated¹⁶, we propose that both coding (e.g. *NRXNI*) and noncoding miR-873-5p variants synergise to increase genetic liability in this ASD case.

Our previous analyses suggested several key ASD-risk genes are likely targets of miR-873 variants¹⁶. We now confirm several risk genes including *ARID1B* and *SHANK3* are regulated by miR-873. Moreover, changes in expression of miR-873 are shown to affect the morphology of neurons and differentiation of SH-SY5Y cells.

Materials and methods

MicroRNA probes

MicroRNA mimics are chemically modified double-stranded RNAs that mimic endogenous miRNAs.

The following microRNA mimics were purchased and employed in this study: wild-type (WT) miRNA-873-5p mimics (5'-GCAGGAACUUGUGAGUCUCCU), mutant (Mut) miRNA-873-5p mimics (5'-GCUGGAACUUGUGAGUCUCCU), control miRNA mimics cel-miR-239b from *C. elegans*, targeting no human genes (5'-UUU GUACUACACAAAAGUACUG), and an inhibitor, anti-sense RNA of miR-873-5p (5'-AGGAGACUCACAA GUUCCUGC) (Dharmacon, Chicago, IL, USA).

Bioinformatic analyses

The targeting genes of WT and Mut miR-873 were pulled down using biotin-conjugated miRNA mimics in SH-SY5Y and the sequencing data have been submitted to GenBank under the Accession number GSE98088¹⁶. Differential gene enrichment between WT and Mut miR-873, and respective controls was calculated with DeSeq2²⁶ as previously described. P values were corrected with the Benjamini–Hocheberg algorithm. Genes were considered as differential targeting if the adjusted P value was <0.01 and absolute fold-enrichment (FE) was ≥ 2 . Gene Ontology (GO) term analysis of differentially enriched genes of WT and Mut miR-873 ($P < 0.01$, $FE \geq 2$) was performed using the Protein ANalysis THrough Evolutionary Relationships (PANTHER) Classification System, version 13.0²⁷. The biological process GO_BP term of WT and Mut miR-873 were further clustered with REVIGO²⁸. The top ten terms were subsequently plotted in GraphPad Prism and relationship of GO_BP terms were visualised using Cytoscape. Pathway and network analyses were conducted with Ingenuity Pathway Analysis (IPA, Qiagen). The list of differentially targeting genes of WT and Mut miR-873 containing gene IDs, fold changes and P values were uploaded into the IPA tool. The WT or Mut miR873 specific targeting genes associated with human diseases were analysed and filtered with "neural disease". Then six autism related diseases: aphasia, speech disorders, cognitive impairment, bipolar disorder, autism and mental retardation were diagrammed in IPA. For the miRNA shared target analysis, the WT miR-873 target genes were uploaded to the IPA software. Then a list containing miR-124, miR-125 and miR-663 was created. The shared gene targets between miR-873 and other miRNAs were compared. To identify the roles of those differentially targeted genes in ASD, we curated critical genes in autism databases SFARI (Simons Foundation)² and Autism KB (the Centre for Bioinformatics, PKU)²⁹.

MiRNA-873 gene targets validation using the dual-luciferase reporter system

The methodological details for this experiment are available in two recent publications from our

laboratory^{30,31}. The dual-luciferase reporter assay (Ψ Check-2 Promega[®]) was used to confirm interactions between miR-873 and miRNA regulatory elements (MREs) of candidate genes in the monkey kidney Cos-7 cell system. First, MREs were predicted with MIR-ANDA³², then ~200–300 bp gene sequence containing MRE was cloned into Ψ Check-2 vector before *Renilla* luciferase (primers were listed in Supplementary Table 1). The expression of *Renilla* luciferase is regulated by the sequences cloned in. The Ψ Check-2 vector also carries a firefly luciferase to monitor the expression levels of the vector in different cells. The constructed vector 1 μ g and miRNA mimics 20 pmol were transfected into Cos-7 cells with Lipofectamine 2000 (Thermo Fischer Scientific, Waltham, MA, USA), the luciferases were allowed to express for 24 h. Then samples were prepared according to the manufacturer's instructions (Promega, Madison, WI, USA). Luciferase activity was measured using a CLARIOstar microplate reader (BMG LABTECH, Germany). The *Renilla*/firefly ratio was calculated, and the percentage of the downregulation was normalised to control cel-miR-293b transfected group. Four independent experiments were conducted.

Gene expression levels measured by qPCR

Gene expression levels were measured with quantitative PCR (qPCR), with the methods reported previously³³. The cells were transfected with 20 pmol each for WT, Mut miR-873 and cel-miR-293b control with Lipofectamine 2000. RNA was extracted with TRIzol reagent (Thermo Fisher Scientific) and reverse transcribed with SuperScript[™] IV First-Strand Synthesis System (Thermo Fisher Scientific), then PCR was performed with QuantiFast SYBR[®] Green PCR Kit (Qiagen) on a LightCycler[®] 480 Instrument (Roche, Switzerland). The expression levels of miR-873 was quantified with the stem-loop RT-PCR method³⁴. GAPDH was used as a control for coding gene and U6 snRNA were used as a control for quantifying miRNA. Four replicates were carried out in each group. All primers were listed in Supplementary Table 1.

Primary neuron culture, transfection, imaging and electrophysiological recording

Primary hippocampal neurons from wild-type (E18) C57BL/6J mice were cultured according to the published protocols³⁵. All the procedures were approved by Monash University Animal Ethics Committee MARP-2 under the approval number MARP/2015/124. The neurons were seeded in a 24-well plate with poly-D-lysine coated glass coverslips at 5×10^4 cells per well. At 11 days in vitro (DIV) culture, the neurons were transfected with 20 pmol each WT, Mut or inhibitors of miR-873 and cel-miR-239b control using the Lipofectamine[®] LTX (Thermo Fischer

Scientific). After 72 h, the neurons were immunostained with dendritic marker Map2 (Abcam, ab5392) and images were taken using Zeiss, AXIO Imager M2 with ZEN software (version 2.0, Germany). Morphology changes (branch number and dendrite length) were graphically and statistically analysed with Image J plugin Sholl analysis³⁶. The number of intersections over the distance from the cell soma, was plotted as a curve for each of the four groups to visualise the average distribution of branches and length of dendrites among four groups. There are more than 60 neurons quantified from each group.

For electrophysiological characterisation of the neurons, coverslips containing transfected neurons were transferred to a recording bath (Warner Instruments, Hamden, CT, USA) and were continuously superfused with physiological saline solution (PSS) containing (mM): NaCl 137, NaHCO₃ 4, NaH₂PO₄ 0.3, KCl 5.4, KH₂PO₄ 0.44, MgCl₂ 0.5, MgSO₄ 0.4, glucose 5.6, HEPES 10, CaCl₂ 1.5 at pH 7.4 at room temperature. Glass electrodes (PG150T-15, Harvard Apparatus, Kent, UK) were pulled (P-97, Sutter Instruments, CA, USA) and fire polished (MG-80, Microforge, Narashige, Japan). The electrodes were filled with solution containing (mM): KCl 10, CaCl₂ 0.05, Mg₂ATP 4, K-gluconate 130, Na₂-phosphocreatine 10, EDTA 0.01, EGTA 0.1, HEPES 10, pH 7.2 and had resistances of 2–5 M Ω . Electrophysiological activity was recorded using the patch-clamp technique in whole-cell mode using an Axopatch 200 A series amplifier (Axon Instruments, CA) controlled by pCLAMP v.10 software (Molecular Devices, San Jose, CA, USA). Data were digitised at 5–20 kHz and analysed using Clampfit 10 (Molecular Devices). Current clamp mode was used to record the resting membrane potential, input capacitance and resistance. Action potentials were evoked using depolarising current steps. Voltage-clamp mode using 10 mV depolarising steps in 10 mV increments, from a holding potential of –100 mV, was used to record voltage-gated inward currents. Tetrodotoxin (TTX) was added to the PSS to block Na⁺ currents (Sigma–Aldrich, St. Louis, MO, USA). Seven neurons in each group were recorded. The preparations were fixed in paraformaldehyde 4% immediately upon termination of electrophysiology and were later stained immunohistochemically.

CRISPR/Cas9 knockout of miR-873 in SH-SY5Y cell

Plasmid pSpCas9(BB)-2A-Puro (PX459) was requested from Dr. Feng Zhang's lab at Broad Institute through Addgene (#62988) and then constructed with protospacer sequences of CRISPR/cas9 against miR-873. The single guide RNA (gRNA) was designed by CRISPR DESIGN (<http://crispr.mit.edu/>)³⁷. The primers for cloning the gRNA sequence were synthesised by Integrated DNA Technologies (Coralville, IA, USA), and then annealed

and cloned into PX459 plasmid. The validated plasmid containing the gRNA sequence and Cas9 was transfected to SH-SY5Y cells with Lipofectamine 2000, and cells were selected with 2 µg/ml puromycin for 6 days. Then single cell was plated into a 96-well plate for proliferation. Cells presented with two different morphologies, the cells with neuronal-like long processes were maintained and Sanger sequencing confirmed. Five potential CRISPR off target genes were confirmed through Sanger sequencing. Anti-βIII tubulin antibody (Abcam, ab18207) was used to indicate the neuron-like feature in those cells with or without miR-873 transfection. The morphology of neurons was further analysed with Sholl analysis, more than 30 neurons were quantified from each group. All primers were listed in Supplementary Table 1.

Statistical analysis

Where required *P* values were adjusted using Benjamini–Hochberg correction for bioinformatics analysis. One-way ANOVA was used for group comparison, and the *P* values for comparison with control groups were obtained from one-way ANOVA; the *P* values for comparison with the effect of WT and Mut miR-873, one-tailed or two-tailed Student's *t*-test was employed. Other statistical analysis was conducted as indicated in the figure legends.

Results

Identification of mRNA targets of WT and Mut miRNA-873

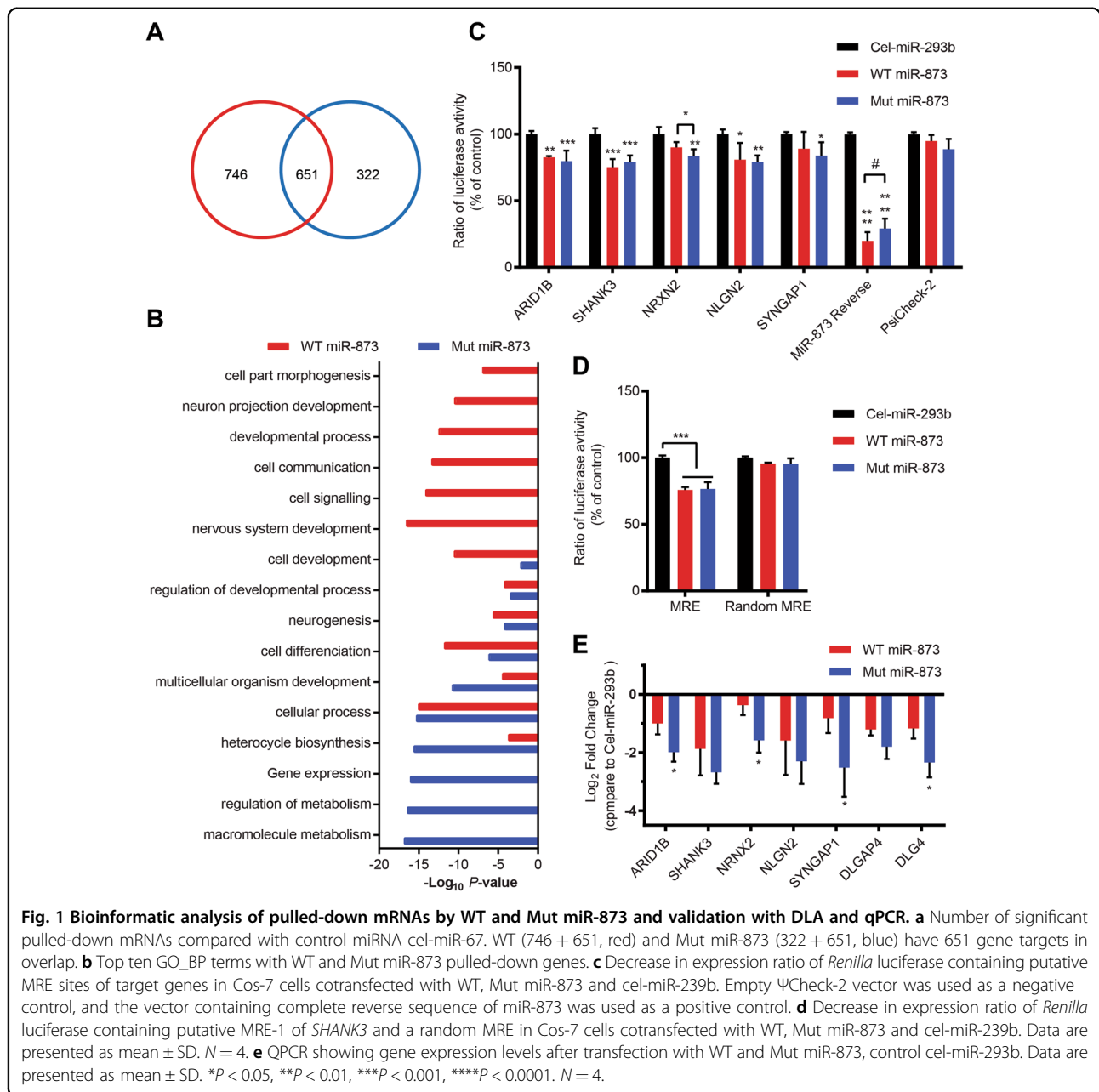
Our previously reported pull-down transcriptome analysis used biotin-conjugated miRNA mimics to identify bound mRNA targets in human neuroblastoma SH-SY5Y cells and results were deposited in GenBank (accession number GSE98088)¹⁶. In contrast with our previous analysis which used $P < 0.05$ ¹⁶, we now use a more rigorous threshold ($P < 0.01$) for choice of candidate target genes of miR-873 for functional analysis. We identified a total of 1719 genes of which 746 are possible unique targets of WT and 322 are unique targets of Mut miR-873, including 651 genes in common [fold enrichment (FE) > 2], indicating a substantial change in the targeting profile (Fig. 1a, Supplementary Fig. 1 and Supplementary Data 1). Gene Ontology_Biological Process (GO_BP) terms were analysed, and the interaction network was created through Cytoscape (Supplementary Data 2). Interestingly, the connections formed within WT miR-873 GO_BP terms are considerably more complex than those formed by Mut miR-873 GO_BP terms (Supplementary Fig. 2). The top ten terms of WT targets are more related with neuronal functions whereas the Mut targets show a relatively nonspecific pattern of biological functions (Fig. 1b) suggesting Mut miR-873 may have lost functions related to binding and regulating genes involved in neurodevelopment including those involved in autism, speech disorders and mental retardation (Table 1).

Among the common targets 37 were associated with the SFARI geneset and 119 with the AutismKB database²⁹, all of which were recognised autism risk genes (Supplementary Fig. 3). Among nonshared target genes, we found 42 (WT-targeted) vs 22 (Mut-targeted) in the SFARI set and WT 119 vs Mut 56 targets in AutismKB (Supplementary Fig. 3), respectively. Notable among these were the chromatin remodelling gene *ARID1B* and synaptic genes *SHANK3* and *NRXN2*. These results indicate one SNV alteration greatly changed the targeting profile and functions of miR-873.

MiR-873 target gene validation using dual-luciferase reporter system

To test whether targeting interactions of miR-873 promote mRNA degradation, we employed a dual-luciferase reporter assay with the Cos-7 cell system as previously described^{31,33,38}. MIRANDA predicted miRNA-873 recognition elements (MREs) were cloned into ΨCheck-2 vector before Renilla luciferase. Targeted *Renilla* luciferase expression was measured against constitutively expressed Firefly luciferase, which was also used as an internal control to monitor transfection efficiency. The empty vector was used as a negative control, and the vector containing miR-873 reverse sequence was used as a positive control. The positive control vector constructed using perfectly matched target sites for miR-873 showed the strongest suppression with $80.0 \pm 2.1\%$ decrease in expression (luminosity) of chimeric *Renilla* luciferase in the presence of the WT miR-873 mimic (Fig. 1c), while the suppression effect was decreased to $70.7 \pm 10.2\%$ with Mut miR-873 confirming a little reduced binding affinity ($P = 0.056$). For cells containing vectors with cloned MREs of *ARID1B*, *SHANK3*, *NRXN2*, *NLGN2* and *SYNGAPI*, WT and Mut miR-873 exerted similar suppression effect on expression of *Renilla* luciferase with decreases of 17.4 ± 6.5 vs $20.4 \pm 9.3\%$; 24.8 ± 13.8 vs $21.1 \pm 10.1\%$; 10.0 ± 1.0 vs $16.5 \pm 5.5\%$; 19.1 ± 8.2 vs $20.9 \pm 10.0\%$; 10.9 ± 10.1 vs $16.1 \pm 5.1\%$, respectively (Fig. 1c). The targeting is significantly different between WT and Mut miR-873 to *NRXN2* with one-tailed Student's *t*-test. To confirm the dysregulation specifically dependent on the MRE within cloned sequences, we compared MRE-1 of *SHANK3* and a randomised MRE sequence (Supplementary Table 2). Results confirmed an inhibition effect for MRE-1 but not for the random sequence for both WT and Mut miR-873 (Fig. 1d). The above results confirmed that miR-873 variants specifically target candidate MRE sequences from those autism risk genes. A ~20% reduction in expression of chimeric *Renilla* luciferase proteins are consistent with levels reported from previous studies using this system^{31,33,38}.

Pull-down RNA sequencing identified differential targeting of WT and Mut miR-873 and the binding and repressing effect of key gene targets were validated using dual-luciferase assay and expression level of ASD-risk



genes measured using quantitative PCR (qPCR) (Fig. 1e). Besides WT and Mut miR-873, control cel-miR-293b mimics with no-known human targets were compared. After transfection with mimics, the mRNA levels of the autism risk genes (i.e. *ARID1B*, *SHANK3*, *SYNGAP1*) and synaptic genes (i.e. *NRXN2*, *DLGAP4*, *DLG4*, *NLGN2*) were found to be downregulated by 2-4 fold in WT and Mut miR-873 compared to cel-miR-293b control. Interestingly, *ARID1B*, *NRXN2*, *SYNGAP1* and *DLG4* were significantly downregulated by Mut miR-873 (Fig. 1e), suggesting a gain-of-function rather than a loss-of-function. Although results confirmed an inhibition effect

of both WT and Mut miRNA-873, Mut miRNA-873 did show a measurable difference in binding affinity to some mRNAs compared to WT and consequently changes in gene expression of those targets. These results more generally indicate miR-873 targets autism risk including key synaptic genes, involved in neurodevelopment and neural function.

MiR-873 effects on neuronal development of mouse primary hippocampal neurons

Mature miR-873-5p is identical in human and mouse. Two MREs of miR-873 in *SHANK3* were identified as

being near identical between human and mouse. Their free energy binding score are -25.41 and -19.15 kCal/mol, respectively (Supplementary Table 2). Targeted dysregulation as implied by dual-luciferase assay (Fig. 1d) suggests miR-873 will regulate human and mouse *SHANK3* transcripts in a similar mode.

To examine the role of miR-873 on neuronal development, we assessed the neuronal morphologies using Sholl analysis³⁶ after transfection with WT, Mut and inhibitor of miR-873 and cel-miR-293b (Fig. 2a). Neurite outgrowth and dendritic branching are critical for the formation and maintenance of the neuronal circuits. The average number of intersections in each group over the distance from the cell soma was calculated and plotted as a curve (Fig. 2b). The number of ramification of neurons in control and WT miR-873 transfected groups was found to be significantly higher than those transfected with miR-873 inhibitor (12.5 ± 4.1 , 12.8 ± 4.2 vs 9.4 ± 4.8 , 9.2 ± 4.2) showing a 25% increase in neuronal complexity/ arborisation (Fig. 2a–c). Notably, the maximum number of intersections in control and WT treated groups was higher than that in both Mut and inhibitor treated groups (Fig. 2b, d). The total intersections being significantly higher in the WT compared to inhibitor group (Fig. 2e). The length of the neuron branches does not show a discernible difference between groups (Fig. 2f). Overall, WT miR-873 was shown to maintain an increased cell complexity with more elaborate arborisation of neurons compared to Mut and inhibitor miR-873 treatments. This in vitro study suggests WT miR-873 has gene regulatory functions associated with neurodevelopment and the Mut miR-873 variant is functionally compromised.

MiR-873 effects on electrophysiological characteristics of primary hippocampal neurons

In current clamp mode, resting membrane potentials of hippocampal neurons transfected with Mut or inhibitor miR-873 were more depolarised than neurons transfected with WT miR-873 (Fig. 3a). The amplitude of the action potential (AP) (Fig. 3b) was significantly larger in mutant miR-873 and inhibitor transfected neurons and this was supported by an enhanced underlying sodium current (Fig. 3c, d). Excitatory postsynaptic potentials (EPSPs) reached threshold for the firing of APs and hence the underlying currents, EPSCs, were studied in the presence of tetrodotoxin (TTX 100 nM) to block APs. EPSCs occurred more frequently in mutant miR-873 and inhibitor transfected neurons (Fig. 3e, f). However, EPSC amplitude was enhanced only in mutant miR-873 neurons (Fig. 3e, g). The frequency of EPSCs was not influenced by blockade of inhibitory neurons with picrotoxin (30 μ M), but they were abolished by CNQX (100 μ M), which blocked AMPA receptors. The results confirm neuronal signalling is changed in mutant miR-873.

Table 1 MIR-873-associated neuronal diseases and function pathways.

Disease	WT miR-873					Mut miR-873				
	Autism	Aphasia	Speech and language disorders	Cognitive impairment	Mental retardation	Bipolar disorder	Mental retardation	Bipolar disorder		
P value	1.82E-02	3.39E-03	5.49E-03	1.67E-02	1.84E-02	1.71E-02	4.15E-03	1.25E-02		
Genes	ACE, HTR6, ACHE, DRD4, GRIN1, MECP2, TCF7L2, GRIN2D	GRN, ACHE, DRD4, GRIN1, GRIN2D	GRN, HTR6, DRD4, ACHE, GRIN1, TCF7L2, GRIN2D, CHAMP1	ACEACHE, ADAT3, ATP1A3, CASP2, CHAMP1, CNNM2, DCX, DRD4, EEF1A2, FASN, GABBR1, GATAD2B, GDI1, LARGE1, GRIN1, GRIN2D, MBOAT7, MECP2, GPC1, TECR, TRAPP9, TSPAN7, MED25, PCYR1, TCF7L2, HTR6, INPP5E, KANSL1,	ADAT3, CASP2, CHAMP1, CNNM2, DCX, MBOAT7, EEF1A2, FASN, GABBR1, MED25, PCYR1, TCF7L2, KANSL1, LARGE1, TECR, GATAD2B, GDI1, GPC1, GRIN1, HTR6, INPP5E, TRAPP9, TSPAN7, DRD4, MECP2, PCYR1, TCF7L2, HTR6, INPP5E, KANSL1,	WHRN, NDUF58, GRIN1, GRIN2D, OGG1, PTPRU, ACHE, ATP1A3, KCNH2, NCS1, DEGS2, DRD4, ABLIM1, ACE, GRM4, HTR6, CHRNB2	CHRM1, CREBBP, SETBP1, T3GAL3, BCL11A, MED12, SIGMAR1, EDC3, ARID1B, EP300, ARID1A, LATS1, SMARCB1, AUTS2	SYN2, SYN3, THRA, EYA3, KCNN3, CHRM1, PRKCA, ZNF490, SLC18A1, SIGMAR1,		

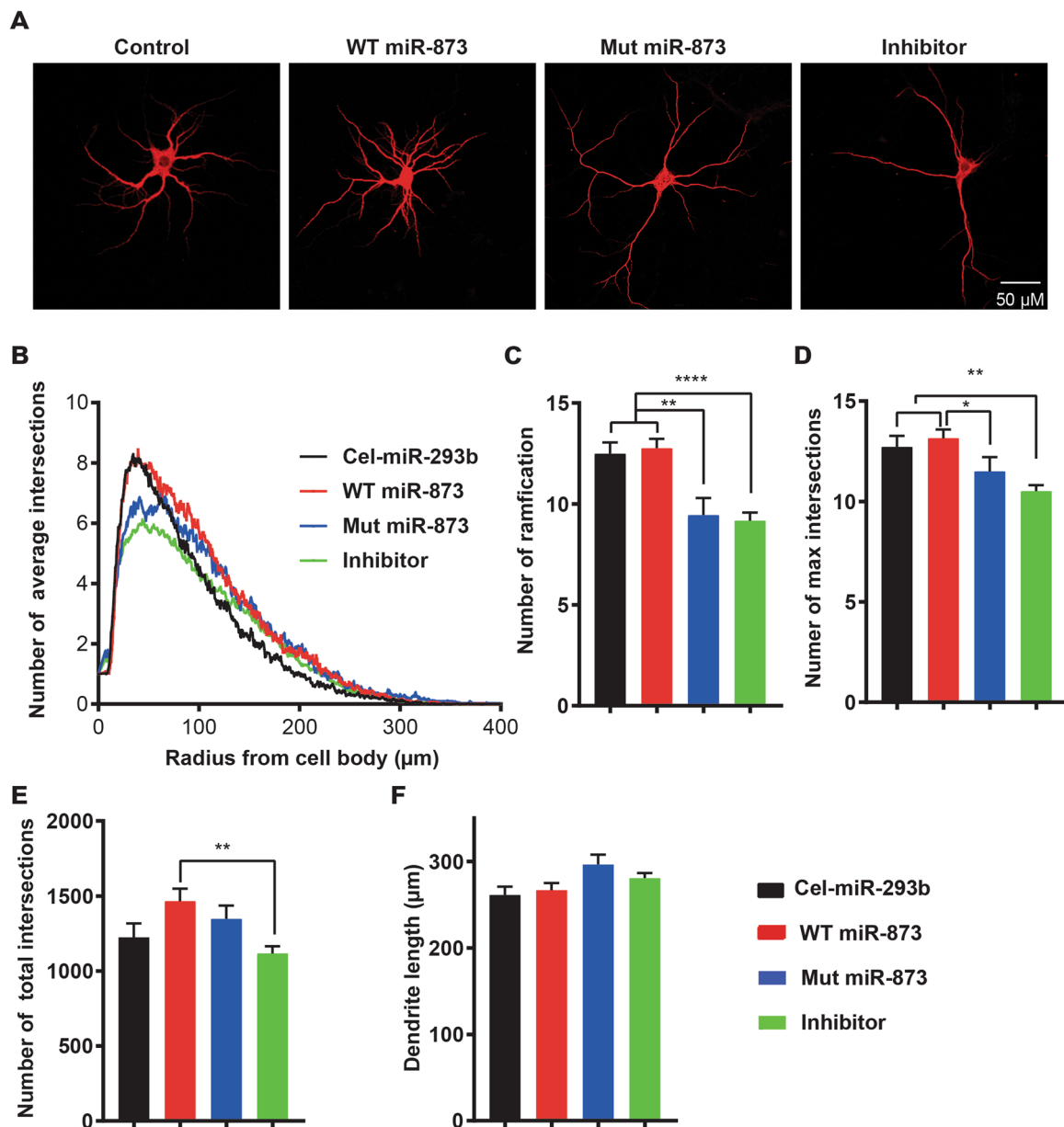
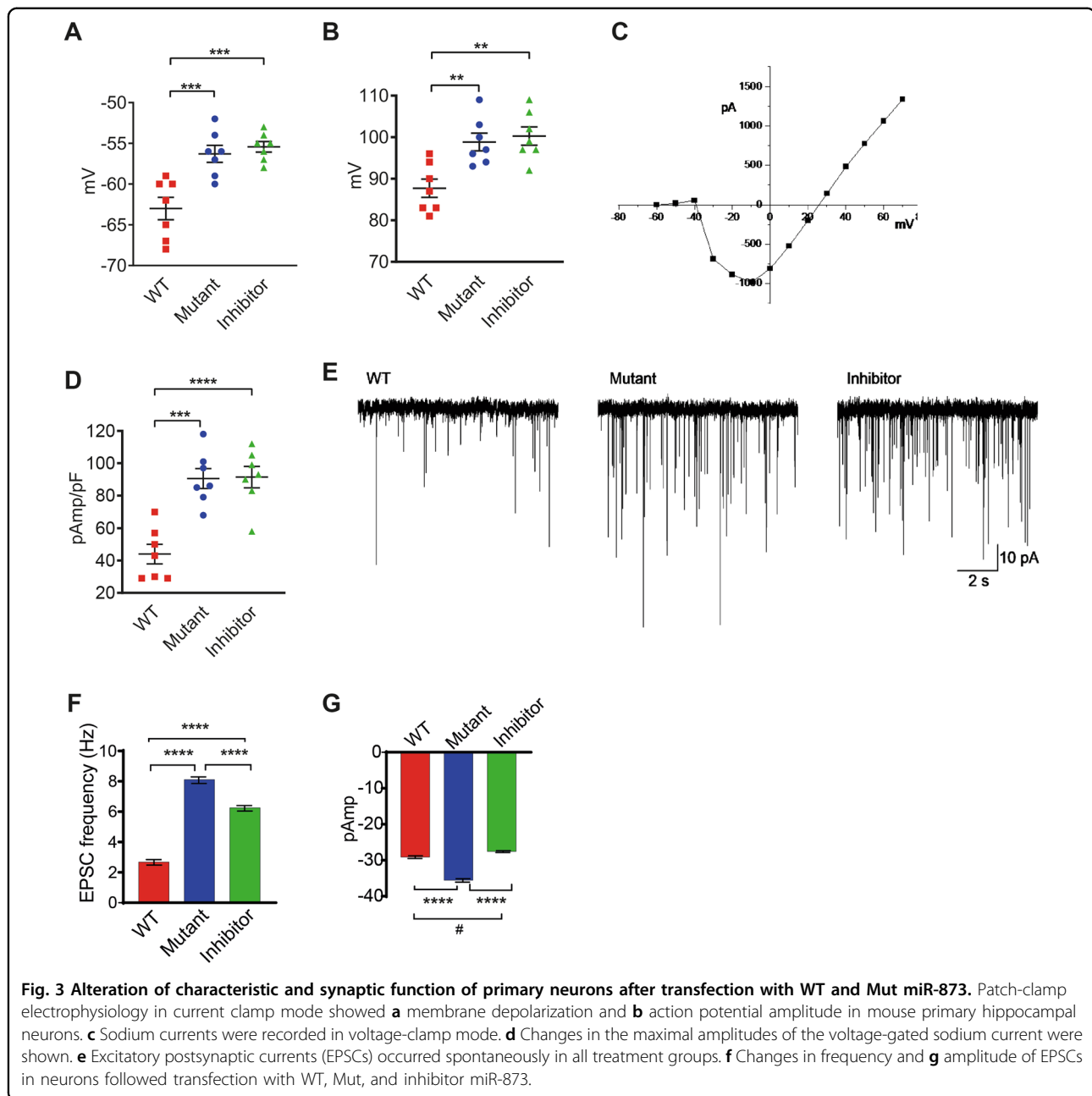


Fig. 2 Morphological changes of primary neurons after transfection with WT and Mut miR-873. **a** Representative images of mouse neurons after transfection with WT, Mut, inhibitor miR-873 and cel-miR-293b. Bar = 50 μm . **b** Number of average intersections on the above four groups analysed with Sholl analysis. **c–f** Number of ramification (**c**), number of max intersections (**d**), number of total intersections (**e**), and dendrite length (**f**), analysed with Sholl analysis. One-way ANOVA was used to compare the WT, Mut miR-873 to the cel-miR-293b group. Data are presented as mean \pm SEM. * $P < 0.05$, ** $P < 0.01$, **** $P < 0.0001$. $N = 60$.

CRISPR/Cas9 knockout of miR-873 in SH-SY5Y cell promoting cell differentiation

To identify roles of miR-873 in cell development, miR-873 was disrupted using CRISPR/Cas9 system, the experimental strategy is shown in Fig. 4a. There were two different cell morphologies after single cell screening, and the ones with neuronal-like longer branches were found to contain miR-873 mutations (Supplementary Fig. 4). Four cell clones were subsequently sequenced and characterised as having various

insertion and deletions (INDELs) that possibly disrupted miR-873 function (Fig. 4b). Sanger sequencing data suggested, clone #1, #3, #4 were potentially result from a biallelic cut, as exhibited a single sequence, while clone #2 was potentially a single allelic mutation with multiple sequences. Clone #1, containing an 18 nt deletion with 12 nt overlapped with miR-873 sequence, was chosen for further analysis. SH-SY5Y cells (control) and miR-873 KO (clone #1) cells were compared. Remarkably, we observed miR-873 KO SH-SY5Y



cells differentiate into a neuronal morphology with marked increase of neurite-like outgrowth without application of transformation factors (e.g. retinoic acid). This neuron-like morphology and differentiation could be suppressed/reversed when cells were transfected with miR-873 for 3 days as shown by β III tubulin stained cells (Fig. 4c). After miR-873 knockout in SH-SY5Y cell, the neurite length had increased from ~ 45 to $123 \mu\text{m}$, and the number of branches increased from ~ 3.8 to 5.1 (Fig. 4d, e). As anticipated, the level of miR-873 expression was greatly reduced in miR-873 KO cells (Fig. 4f); whereas the expression levels of miR-873 targeted genes (e.g. *ARID1B*, *SHANK3*, *ADNP2*, *ANK2* and *CHD8*)

were conversely upregulated (Fig. 4g). We note that *ADNP2*, *CDH8* and *ARID1B* have functions related to transcription and chromosome remodelling^{39–41}. These data suggest miR-873 may function to suppress neuronal differentiation.

Discussion

Using whole-exome sequencing, our laboratory has identified many rare SNVs (mutations) in the functional binding regions (seed sequence) of miRNAs in ASD patients, suggesting these miRNAs play important roles in ASD development^{5,16}. Among these was a rare SNV mutation (rs777143952: T > A) associated with

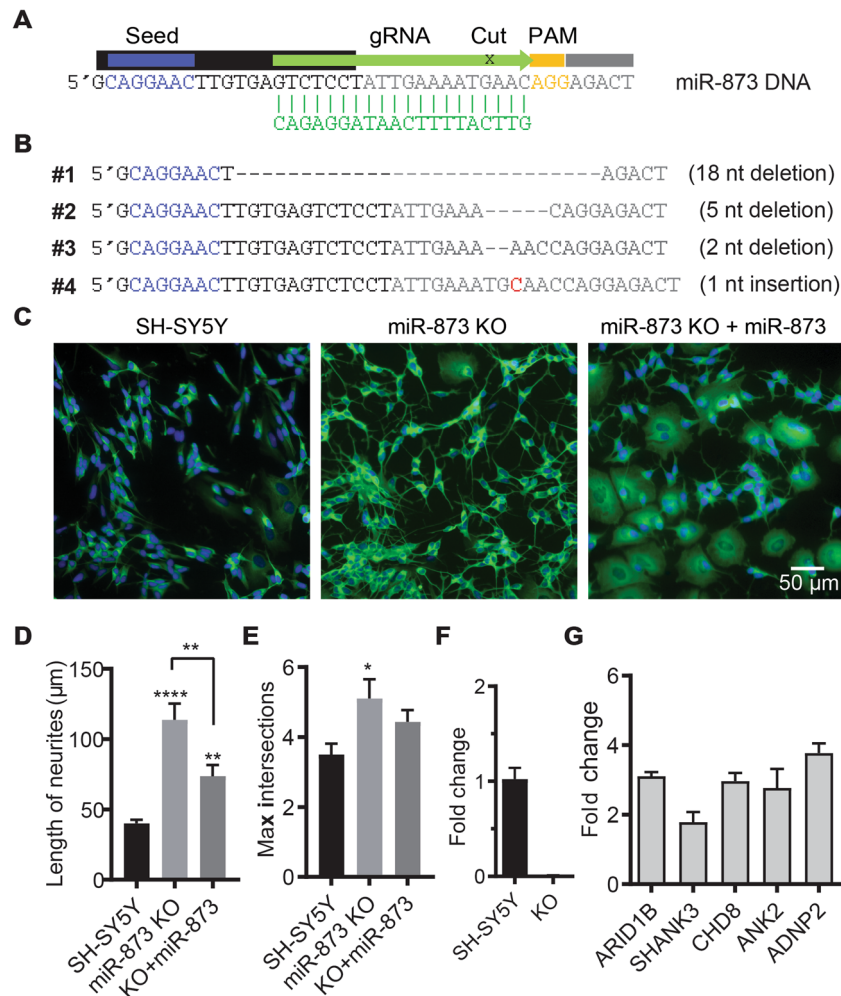


Fig. 4 CRISPR/Cas9 MiR-873 knockout in SH-SY5Y cells. **a** Design of guide RNA (gRNA) used for the CRISPR/Cas9 genome editing. PAM sequence, orange; gRNA, green; miR-873 mature sequence, black; seed, blue. **b** CRISPR/Cas9 generated indels in four miR-873 gene disrupted cell clones. **c** β III tubulin staining of 6-day cultured control (SH-SY5Y) cells, miR-873 KO (clone #1) and WT miR-873 mimics transfected cells (clone #1 + WT miR-873). **d** Neurite length and number of max intersections (**e**) were analysed with Sholl analysis. Data are presented as mean \pm SEM. * $P < 0.05$, *** $P < 0.01$, **** $P < 0.0001$. $N = 30$. **f** QPCR confirmed loss of miR-873 expression in KO cells. U6 snRNA was used as an internal control. $N = 3$. **g** Expression levels of candidate ASD genes in miR-873 KO cells. GAPDH was used as an internal control. Data are presented as mean \pm SD. $N = 3$.

mature miR-873 gene, which is highly expressed in human brain. We subsequently conducted a pull-down transcriptome analysis to identify miR-873 targets in a human neuroblastoma cell line SH-SY5Y. Among the genes differentially targeted by WT and Mut miR-873 were notable ASD-risk genes *ARID1B*, *SHANK3* and *NRXN2*. In this study, we experimentally validated differential targeted genes of WT and Mut miR-873 using dual-luciferase assay and qPCR. We examined changes in morphology and the excitability of primary cultured neurons with transfection of WT and Mut miR-873. We also identified a role of miR-873 in repressing neuronal differentiation with CRISPR/Cas9 gene knockout.

Although cultured SH-SY5Y cells do not reflect *in vivo* conditions of neurons, they express many neural genes^{42–44}, hence they were specifically useful as a 'mechanistic model' to examine binding affinity and changes in expression of known ASD-risk genes at measurable levels¹⁷. Autism risk genes, *ARID1B*, *SHANK3* and *NRXN2* were specially of interest, using a dual-luciferase assay we confirmed the direct targeting of MRE of *SHANK3* by miR-873 albeit, WT and Mut miR-873 mimics similarly dysregulate *Renilla* luciferase. *ARID1B* mutations previously reported in autism cases^{45,46} also cause autistic-like behaviours in mouse models⁴⁷. Same as with *SHANK3*, targeting *ARID1B* by WT and Mut miR-873 reduced *Renilla* chimeric luciferase expression at similar levels. Like *NRXN1*, *NRXN2* has a

direct genetic association with ASD¹⁷, it is a major contributor to synapse development and changes to its expression, as suggested by our results, may affect synaptic homeostasis. Gene transcripts often contain multiple MREs with slight differences in sequence homology and arguably different binding affinity (e.g. *SHANK3*, Supplementary Table 2) including sites found in introns and alternate spliced gene variants that may independently or together affect mRNA dysregulation. All these target sites would need to be exhaustively tested to determine specific molecular differences between WT and Mut miR-873 in vitro, as reflected by changes to gene expression (Fig. 1e).

Transfection of the mutant miR-873 or inhibitor had significant effects on the morphology properties of primary hippocampal neurons assessed by Sholl analysis. MiR-873 transfected primary hippocampal neurons maintain branches and ramifications similar to control neurons, while mutant/inhibitor transfections resulted in less neuronal complexity (Fig. 2). MiR-873 dysregulated key neural genes including *SHANK3* (Fig. 1c–e) leading to observable changes in the development of cultured primary neurons that reflect previously reported results⁴.

Transfection of the mutant or inhibitor miR-873 had significant effects on the functional properties of primary hippocampal neurons assessed electrophysiologically. Membrane potential was significantly depolarised by 7 mV. Importantly, this standing depolarisation has implications for voltage-gated ion channel function. For example, it would be expected to induce ongoing inactivation of the voltage-gated sodium channels responsible for the upstroke and amplitude of the AP. In contrast to expectations, the amplitude of the AP was enhanced as a result of miR-873 transfection (Fig. 3b). Then, using voltage-clamp mode, an increase in the sodium current was observed and this explains the increase in the amplitude of the AP (Fig. 3d). The depolarisation likely reflects effects on ion channel expression. Shanks, Neuroligins and Neurexins are involved in the development of the synapse, both pre- and postsynaptically and this includes cytoskeletal support for various ion channels and transmitter receptors⁴⁸. Overexpression of *NLGNI* results in an increase in spontaneous EPSC frequency in mouse hippocampal neurons⁴⁹ and this supports the interpretation similar to our observation that miR-873 has a suppressor function, albeit decreasing *NLGNI* increased transmitter release in hippocampus and this could not be rescued by *NLGNI*⁵⁰. Clearly, further investigation is required if we are to fully understand this system. Our results support the notion that miR-873 may negatively regulate translation of these proteins and reduction/removal of this miRNA results in enhanced synaptic activity. This effect was abolished by overexpression of Mut miR-873 or inhibitor.

To further explore the biological function of miR-873 on cell development, we genetically disrupted miR-873 using the CRISPR/Cas9 system in human SH-SY5Y cells. Several clones containing INDELS were generated near the cutting site, the resultant miR-873 KO cells were remarkable because they spontaneously differentiated into neuronal-like cells without application of transformation factors (Fig. 4c and Supplementary Fig. 4). We also sequenced putative clones with normal SH-SY5Y cell morphology, confirming they did not contain any mutations flanking the miR-873 gene. Interestingly, clone #2 cells that showed morphological changes contained a single allelic mutation (heterozygous), similar to the genetic profile of the proband associated with this mutation, indicating possible haploinsufficiency in these cells. Among clones that affected cell phenotype, clone #1 was chosen for further study due to a sizeable 12 nt deletion of miR-873 mature sequence (22 nt) (Fig. 4b). The functional knockout status of clone #1 was characterised in increased expression of ASD-risk genes normally targeted by miR-873. Three genes *ADNP2*, *ARID1B* and *CHD8* are known to be involved in transcription control and cell differentiation^{39–41} while *ANK2* has been shown to bind reversibly to the cytoplasmic domain of L1CAM and mediate linkage to the spectrin-actin cytoskeleton related to axon sprouting and neuronal morphology⁵¹. Quantitative PCR showed >2-folds increase in expression of selected ASD genes in KO compared to control cells, a result that is commensurate with target enrichment levels observed in SH-SY5Y pull-down results¹⁶ (Fig. 4g). This suggests miR-873 may act as a repressor of cell differentiation similar to other miRNAs. For instance, miR-124 and miR-125b overexpression has been shown to increase neuronal differentiation^{6,52}, while miR-663 represses neuronal differentiation⁵³ an observation that resonates with our own result. We also observed 21.4% (301) of genes targeted by miR-873¹⁶ are also targets of miR-663 while only 8.3% (117) genes are shared targets with miR-124 (Supplementary Data 3).

Considering the spatiotemporal functions of miR-873 are yet to be defined, comparing phenotypes in very different cells can be misleading. We note the role miR-873 plays in repressing neuronal-like differentiation and its absence promoting neurite-like outgrowth in neuroblastoma cells is counterintuitive with overexpression of miR-873 increasing complexity in primary mouse neurons. Irrespective of conflicting phenotypes miR-873 likely acts as a switch during development. Whether it is ON or OFF will depend on the molecular environment. In neuroblast cells the molecular configuration might be altered or reflect a role tuned to early development, as determined by molecular targets available for interaction. It is also important to reflect on the genomic context of miR-873 being located within an intron of the neural gene

LINGO2. We are aware of a number of reported copy number variations of *LINGO2* found in autism cases^{54,55} including ones which disrupt miR-873^{56,57}. Considering miR-873 may be co-regulated with *LINGO2*, this gene complex warrants further investigation.

Evidently, miRNAs are configured by evolution to control networks of genes whose expression is triggered during a developmental/functional program or through environmental cues. Understanding how these different noncoding regulatory genes work in parallel to shape genetic expression during development and cell differentiation remains a major challenge for cell biology.

Notwithstanding the miR-873-5p variant was inherited from an unaffected parent, we consider how this rare mutation might additively contributed to ASD risk by overlaying other DNA variations to influence genetic liability in this case. The measurable loss of binding and differential expression of several autism risk genes when combined with the mutation load from the mother with recorded BAP¹⁶ is particularly relevant. Consistent with this idea is the functional disruption of the neurexin-neurexin axis in this individual—specifically a putative shift in miR-873 binding affinity involving a number of synaptic genes (*NRXN2*, *NLGN2*, *-3*, *-4X*, *DLG4*, *DLGAP3*, *-4* and *SHANK1*, *-2*, *-3*) when combined with the loss of function *NRXN1* coding variant^{5,16}. Future mouse KO studies whereby combinations of coding and noncoding variants are placed in the same genetic background will directly address this question. Alternately, the CRISPR/Cas9 system could be used to examine combinations of variants in human induced pluripotent stem (iPS) cells.

In summary our results represent the first functional evidence that miR-873 regulates genes associated with changes in neuronal morphology and cell differentiation that builds upon the association with and significance to autism spectrum disorder.

Acknowledgements

We acknowledge the financial support from Australian National Health and Medical Research Council (APP1008125). We thank Monash bioinformatics platform for providing bioinformatics support.

Author details

¹Monash Biomedicine Discovery Institute, Monash University, Melbourne, VIC 3800, Australia. ²Monash Bioinformatics Platform, Monash University, Melbourne, VIC 3800, Australia. ³Queensland Brain Institute, The University of Queensland, Brisbane, QLD 4072, Australia. ⁴Centre for Mental Health Research, The Australian National University, Canberra, ACT 0200, Australia

Conflict of interest

The authors declare that they have no conflict of interest.

Publisher's note

Springer Nature remains neutral with regard to jurisdictional claims in published maps and institutional affiliations.

Supplementary Information accompanies this paper at (<https://doi.org/10.1038/s41398-020-01106-8>).

Received: 1 October 2019 Revised: 21 October 2020 Accepted: 17 November 2020

Published online: 01 December 2020

References

- Huguet, G., Ey, E. & Bourgeron, T. The genetic landscapes of autism spectrum disorders. *Annu. Rev. Genomics Hum. Genet.* **14**, 191–213 (2013).
- Basu, S. N., Kollu, R. & Banerjee-Basu, S. AutDB: a gene reference resource for autism research. *Nucleic Acids Res.* **37**, D832–D836 (2009).
- O'Roak, B. J. et al. Sporadic autism exomes reveal a highly interconnected protein network of de novo mutations. *Nature* **485**, 246–250 (2012).
- Peca, J. et al. Shank3 mutant mice display autistic-like behaviours and striatal dysfunction. *Nature* **472**, 437–442 (2011).
- An, J. Y. et al. Towards a molecular characterization of autism spectrum disorders: an exome sequencing and systems approach. *Transl. Psychiatry* **4**, e394 (2014).
- Makeyev, E. V., Zhang, J., Carrasco, M. A. & Maniatis, T. The MicroRNA miR-124 promotes neuronal differentiation by triggering brain-specific alternative pre-mRNA splicing. *Mol. Cell.* **27**, 435–448 (2007).
- Amaral, P. P. & Mattick, J. S. Noncoding RNA in development. *Mamm. Genome* **19**, 454–492 (2008).
- Mattick, J. S. & Mehler, M. F. RNA editing, DNA recoding and the evolution of human cognition. *Trends Neurosci.* **31**, 227–233 (2008).
- Cheng, C., Bhardwaj, N. & Gerstein, M. The relationship between the evolution of microRNA targets and the length of their UTRs. *BMC Genomics* **10**, 431 (2009).
- Güven-Ozkan, T. et al. MiR-980 is a memory suppressor microRNA that regulates the autism-susceptibility gene A2bp1. *Cell Rep.* **14**, 1698–1709 (2016).
- Ghahramani Seno, M. M. et al. Gene and miRNA expression profiles in autism spectrum disorders. *Brain Res.* **1380**, 85–97 (2011).
- Vaishnavi, V., Manikandan, M. & Munirajan, A. K. Mining the 3'UTR of autism-implicated genes for SNPs perturbing microRNA regulation. *Genomics Proteom. Bioinforma.* **12**, 92–104 (2014).
- Devanna, P. & Vernes, S. C. A direct molecular link between the autism candidate gene RORa and the schizophrenia candidate MIR137. *Sci. Rep.* **4**, 3994 (2014).
- Xu, B., Hsu, P. K., Karayiorgou, M. & Gogos, J. A. MicroRNA dysregulation in neuropsychiatric disorders and cognitive dysfunction. *Neurobiol. Dis.* **46**, 291–301 (2012).
- Rana, T. M. Illuminating the silence: understanding the structure and function of small RNAs. *Nat. Rev. Mol. Cell Biol.* **8**, 23–36 (2007).
- Williams, S. M. et al. An integrative analysis of non-coding regulatory DNA variations associated with autism spectrum disorder. *Mol. Psychiatry* **24**, 1707–1719 (2019).
- Gauthier, J. et al. Truncating mutations in NRXN2 and NRXN1 in autism spectrum disorders and schizophrenia. *Hum. Genet.* **130**, 563–573 (2011).
- Liu, Y. et al. Mutation analysis of the NRXN1 gene in a Chinese autism cohort. *J. Psychiatr. Res.* **46**, 630–634 (2012).
- Wisniewicka-Kowalik, B. et al. Intragenic rearrangements in NRXN1 in three families with autism spectrum disorder, developmental delay, and speech delay. *Am. J. Med. Genet. B Neuropsychiatr. Genet.* **153B**, 983–993 (2010).
- Haines, B. P. & Rigby, P. W. Expression of the Lingo/LERN gene family during mouse embryogenesis. *Gene Expr. Patterns* **8**, 79–86 (2008).
- Ziats, M. N. & Rennert, O. M. Identification of differentially expressed microRNAs across the developing human brain. *Mol. Psychiatry* **19**, 848–852 (2014).
- Karczewski, K. et al. Variation across 141,456 human exomes and genomes reveals the spectrum of loss-of-function intolerance across human protein-coding genes. *BioRxiv* <https://doi.org/10.1101/531210> (2019).
- Kozomara, A., Birgaoanu, M. & Griffiths-Jones, S. miRBase: from microRNA sequences to function. *Nucleic Acids Res.* **47**, D155–D162 (2019).
- Wang, R. J. et al. MicroRNA-873 (miRNA-873) inhibits glioblastoma tumorigenesis and metastasis by suppressing the expression of IGF2BP1. *J. Biol. Chem.* **290**, 8938–8948 (2015).
- Koufaris, C. et al. Haploinsufficiency of the miR-873/miR-876 microRNA cluster is associated with craniofacial abnormalities. *Gene* **561**, 95–100 (2015).
- Love, M. I., Huber, W. & Anders, S. Moderated estimation of fold change and dispersion for RNA-seq data with DESeq2. *Genome Biol.* **15**, 550 (2014).
- Mi, H., Muruganujan, A. & Thomas, P. D. PANTHER in 2013: modeling the evolution of gene function, and other gene attributes, in the context of phylogenetic trees. *Nucleic Acids Res.* **41**, D377–D386 (2013).

28. Supek, F., Bosnjak, M., Skunca, N. & Smuc, T. REVIGO summarizes and visualizes long lists of gene ontology terms. *PLoS ONE* **6**, e21800 (2011).
29. Xu, L. M. et al. AutismKB: an evidence-based knowledgebase of autism genetics. *Nucleic Acids Res.* **40**, D1016–D1022 (2012).
30. Cristino, A. S. et al. Neurodevelopmental and neuropsychiatric disorders represent an interconnected molecular system. *Mol. Psychiatry* **19**, 294–301 (2014).
31. Joilin, G. et al. Rapid regulation of microRNA following induction of long-term potentiation in vivo. *Front Mol. Neurosci.* **7**, 98 (2014).
32. Enright, A. J. et al. MicroRNA targets in Drosophila. *Genome Biol.* **5**, R1 (2003).
33. Cristino, A. S. et al. Neuroligin-associated microRNA-932 targets actin and regulates memory in the honeybee. *Nat. Commun.* **5**, 5529 (2014).
34. Chen, C. et al. Real-time quantification of microRNAs by stem-loop RT-PCR. *Nucleic Acids Res.* **33**, e179 (2005).
35. Kaech, S. & Banker, G. Culturing hippocampal neurons. *Nat. Protoc.* **1**, 2406–2415 (2006).
36. Binley, K. E., Ng, W. S., Tribble, J. R., Song, B. & Morgan, J. E. Sholl analysis: a quantitative comparison of semi-automated methods. *J. Neurosci. Methods* **225**, 65–70 (2014).
37. Ran, F. A. et al. Genome engineering using the CRISPR-Cas9 system. *Nat. Protoc.* **8**, 2281–2308 (2013).
38. Watts, M. E., Williams, S. M., Nithianantharajah, J. & Claudianos, C. Hypoxia-induced microRNA-210 targets neurodegenerative pathways. *Noncoding RNA* **4**, 10 (2018).
39. Ka, M., Chopra, D. A., Dravid, S. M. & Kim, W. Y. Essential roles for ARID1B in dendritic arborization and spine morphology of developing pyramidal neurons. *J. Neurosci.* **36**, 2723–2742 (2016).
40. Malishkevich, A., Leyk, J., Goldbaum, O., Richter-Landsberg, C. & Gozes, I. ADNP/ADNP2 expression in oligodendrocytes: implication for myelin-related neurodevelopment. *J. Mol. Neurosci.* **57**, 304–313 (2015).
41. Zhao, C. et al. Dual requirement of CHD8 for chromatin landscape establishment and histone methyltransferase recruitment to promote CNS myelination and repair. *Dev. Cell* **45**, 753–768.e758 (2018).
42. Lu, J., Li, T., He, R., Bartlett, P. F. & Gotz, J. Visualizing the microtubule-associated protein tau in the nucleus. *Sci. China Life Sci.* **57**, 422–431 (2014).
43. Lu, J., Shu, R. & Zhu, Y. Dysregulation and dislocation of SFPQ disturbed DNA organization in Alzheimer's disease and frontotemporal dementia. *J. Alzheimers Dis.* **61**, 1311–1321 (2018).
44. Krishna, A. et al. Systems genomics evaluation of the SH-SY5Y neuroblastoma cell line as a model for Parkinson's disease. *BMC Genomics.* **15**, 1154 (2014).
45. Hoyer, J. et al. Haploinsufficiency of ARID1B, a member of the SWI/SNF-a chromatin-remodeling complex, is a frequent cause of intellectual disability. *Am. J. Hum. Genet.* **90**, 565–572 (2012).
46. Halgren, C. et al. Corpus callosum abnormalities, intellectual disability, speech impairment, and autism in patients with haploinsufficiency of ARID1B. *Clin. Genet.* **82**, 248–255 (2012).
47. Shibutani, M. et al. Arid1b haploinsufficiency causes abnormal brain gene expression and autism-related behaviors in mice. *Int. J. Mol. Sci.* **18**, e1872 (2017).
48. Sudhof, T. C. Towards an understanding of synapse formation. *Neuron* **100**, 276–293 (2018).
49. Wittenmayer, N. et al. Postsynaptic Neuroligin1 regulates presynaptic maturation. *Proc. Natl Acad. Sci. USA* **106**, 13564–13569 (2009).
50. Polepalli, J. S. et al. Modulation of excitation on parvalbumin interneurons by neuroligin-3 regulates the hippocampal network. *Nat. Neurosci.* **20**, 219–229 (2017).
51. Schafer, M. K. & Frotscher, M. Role of L1CAM for axon sprouting and branching. *Cell Tissue Res.* **349**, 39–48 (2012).
52. Le, M. T. et al. MicroRNA-125b promotes neuronal differentiation in human cells by repressing multiple targets. *Mol. Cell Biol.* **29**, 5290–5305 (2009).
53. Shu, R. et al. APP intracellular domain acts as a transcriptional regulator of miR-663 suppressing neuronal differentiation. *Cell Death Dis.* **6**, e1651 (2015).
54. Pinto, D. et al. Functional impact of global rare copy number variation in autism spectrum disorders. *Nature* **466**, 368–372 (2010).
55. Gazzellone, M. J. et al. Copy number variation in Han Chinese individuals with autism spectrum disorder. *J. Neurodev. Disord.* **6**, 34 (2014).
56. Marshall, C. R. & Scherer, S. W. Detection and characterization of copy number variation in autism spectrum disorder. *Methods Mol. Biol.* **838**, 115–135 (2012).
57. Sanders, S. J. et al. De novo mutations revealed by whole-exome sequencing are strongly associated with autism. *Nature* **485**, 237–241 (2012).